Tracking the Chemistry of Unsaturated C3H3 Groups Adsorbed on a Silver Surface: Propargyl–Allenyl–Acetylide Triple Bond Migration, Self-Hydrogenation, and Carbon–Carbon Bond Format...

ARTICLE *in* JOURNAL OF THE AMERICAN CHEMICAL SOCIETY · JULY 2008

Impact Factor: 12.11 · DOI: 10.1021/ja803509y · Source: PubMed

J|A|C|S
ARTICLES

Published on Web 07/10/2008

Tracking the Chemistry of Unsaturated C_3H_3 Groups Adsorbed on a Silver Surface: Propargyl−Allenyl−Acetylide Triple Bond Migration, Self-Hydrogenation, and Carbon−Carbon Bond Formation

Hsuan Kung,[†] Shin-Mou Wu,[†] Yu-Jui Wu,[†] Yaw-Wen Yang,[‡] and Chao-Ming Chiang*,[†]

Department of Chemistry, Center for Nanoscience and Nanotechnology, National Sun Yat-Sen University, Kaohsiung, Taiwan 80424, and National Synchrotron Radiation Research Center (NSRRC), Hsinchu, Taiwan 30077

Received May 12, 2008; E-mail: cmc@mail.nsysu.edu.tw

Abstract: A diverse array of unsaturated C_1 (methylene and methylidyne) and C_2 (vinyl, vinylidene, ethylidene, and ethylidyne) bound to metal center(s) and surfaces has received much attention. In sharp contrast to the effort devoted to C_1 and C_2 ligands, complexes or surfaces bearing C_3 fragments have been less explored, especially the $M-C_3H_3$ systems, which include propargyl ($M-CH_2C\equiv CH$), allenyl ($M-CH=C=CH_2$), and acetylide ($M-C\equiv CCH_3$) forms. To understand the bonding and reactivity of these C_3 species appended to an extended metal structure, proprargyl bromide ($Br-CH_2C\equiv CH$) was utilized as a precursor to generate C_3H_3 fragments on a Ag(111) surface under ultrahigh vacuum conditions. The molecular transformation process was explored by a combination of temperature-programmed desorption (TPD), reflection absorption infrared spectroscopy (RAIRS), and X-ray photoemission spectroscopy (XPS) techniques. In addition, density functional theory (DFT) calculations were conducted to obtain the optimized geometries and energies for the various surface intermediates. The computed IR spectra facilitated the vibrational mode assignments. TPD spectra show that $C_3H_{3(ad)}$ self-hydrogenates to C_3H_4 around 300 and 475 K, respectively. In addition to hydrogenation, a C−C coupling product C_6H_6 (2,4-hexadiyne) is also unveiled as part of the desorption feature at 475 K. Identification of the possible C_3H_4 isomers (propyne and/or allene) was equivocal, but it was circumvented by using an α,α-dimethyl-substituted propargylic species $-(CH_3)_2{}^{\alpha}C-C\equiv CH$, which results in hydrogenatioin products, alkynic $(CH_3)_2CH-C\equiv CH$ and allenic $(CH_3)_2C=C=CH_2$, distinguishable by the mass spectrometry. The substitution experiments clarify that in the normal case the convoluted TPD feature around 300 K, in fact, consists of both allene at 260 K and propyne at 310 K, while the last hydrogenation product at 475 K is solely propyne. The RAIR spectroscopy demonstrates that at 200 K $C_3H_{3(ad)}$ on Ag(111) readily adopts the allenyl formalism involving concerted C−Br bond scission and [1,3]-sigmatropic migration (i.e., $Br-{}^*CH_2C\equiv CH \rightarrow {}^*CH_2=C=CH-Ag$), in which the σ bond moves to a new metal location across the π-periphery. Single hydrogen incorporation to the α-carbon of the surface allenyl rationalizes the allene formation at 260 K. When the surface is heated to the range of 250−300 K, both RAIR and XP spectra reveal drastic changes, indicative of a new species whose spectral characteristics could be duplicated by separate measurements from 1-propyn-1-yl iodide ($CH_3-C\equiv C-I$) being a direct source for the surface methylacetylide ($CH_3-C\equiv C-Ag$). It is thus suggested that allenyl is further reorganized to render acetylide presumably via [1,3]-hydrogen shift (i.e., ${}^*CH_2=C=CH-Ag \rightarrow {}^*CH_3-C\equiv C-Ag$). The presence of this third $Ag-C_3H_3$ isomeric form demonstrates an unprecedented propargyl−allenyl−acetylide multiple rearrangements on a metal surface. Migration of the triple bond from the remote terminal position into the chain, through the stage of allenic structure, is driven by thermodynamic stabilities, supported by the DFT total energy calculations. Consequently, the evolutions of propyne at 310 and 475 K, as well as 2,4-hexadiyne (bismethylacetylide), can all be reasoned out.

1. Introduction

C_3H_3 represents one of the simplest conjugated organic free radicals, including two linear isomeric forms, $^{\bullet}CH_2-C\equiv CH$ (2-propynyl or propargyl) and $^{\bullet}C\equiv C-CH_3$ (1-propynyl). The propargyl radical is generally considered to be a resonance hybrid of the propargylic $^{\bullet}CH_2-C\equiv CH$ and the allenic $^{\bullet}CH=C=CH_2$ structures. Here, the propargylic form is universally accepted to be the lowest energy isomer.[1] The attachment of the C_3H_3 to the metal is also interesting. For example, among

[†] National Sun Yat-Sen University.
[‡] NSRRC.

(1) Wheeler, S. E.; Robertson, K. A.; Allen, W. D.; Schaefer, H. F., III; Bomble, Y. J.; Stanton, J. F. *J. Phys. Chem. A* **2007**, *111*, 3819–3830.

10.1021/ja803509y CCC: $40.75

the various monolithiated C_3H_3Li reagents, the acetylide structure, Li—C≡C—CH_3, was found to be the most stable.[2] The equilibrating propargyl−allenyllithium reagents (Li—CH_2—C≡CH ↔ Li—CH=C=CH_2) show an inherent bias toward the allenyl form.[3] As ligands in transition-metal complexes, propargyl and allenyl, via σ and/or π interactions, possess diverse bonding modes concomitant with intriguing reactivities.[4] A metal−allenyl bond is believed to be stronger than a metal−propargyl bond.[5] Metal η^1-propargyl and η^1-allenyl complexes (L_nM—CH_2—C≡CH and L_nM—CH=C=CH_2, M and L stand for metal and ancillary ligands, respectively) are tautomeric species, and two pathways have been considered for their interconversion: [1,3]-hydrogen and [1,3]-metal migration, where a polyhapto-bound form, the η^3-propargyl/allenyl, has often been suggested as the intermediate in their mutual isomerization.[6] By contrast, the acetylide species (L_nM—C≡C—CH_3) has no analogous resonance stabilization; thus, internal bond rearrangement is not expected. Surface is an extended metal structure; therefore, it can be viewed as multinuclear. Metal surface-bonded C_3H_3, because of the added chemical dimensions in which adjacent metal centers can act in a cooperative manner, may display chemistry that differs appreciably from the single-metal counterparts. Despite the potentially wealthy chemistry, surface studies on the bonding and reactivity of C_3H_3 remain scarce.

An elegant entry to the topic was pioneered by Barteau and co-workers, in the context of surface acid−base reactions (the surface acts as a solid base), elucidating that propyne (CH_3—C≡CH) adsorbed dissociatively on a ZnO surface via abstraction of a methyl proton to form propargyl species exclusively,[7,8] while removal of the acetylenic proton was favored by oxygen atoms on a Ag(110) surface, resulting in methylacetylide intermediates.[9] Recent studies from our laboratory reported isolation and identification of surface allenyl and methylacetylide, respectively, on Ag(111) by using propargyl bromide[10] and 1-propyn-1-yl iodide[11] as precursors. Here, we present a comprehensive study using temperature-programmed desorption (TPD), reflection absorption infrared spectroscopy (RAIRS), X-ray photoemission spectroscopy (XPS), and density functional theory (DFT) calculations to track the detailed molecular transformations and reaction pathways of chemisorbed C_3H_3 moieties on a Ag(111) surface. When the chemistry is initiated with a 2-propynyl precursor (propargyl bromide, Br—CH_2—C≡CH), the organic C_3H_3 part is found to readily present itself in the tautomeric allenyl formalism on the surface upon rupturing the C—Br bond at 200 K. It is even more intriguing that this allenyl structure can further convert into methylacetylide intermediacy at 250 K, confirmed independently by using a 1-propynyl precursor (1-propyn-1-yl iodide, I—C≡C—CH_3). Such a cascade of internal bond rearrangement steps (propargyl−allenyl−methylacetylide) manifests that the alkynic C≡C functionality in a MCCC framework has the propensity to migrate from the terminal position, via a cumulated double-bond middle stage, into the hydrocarbon chain for a closer proximity to the metal surface. During the consecutive isomerization processes, C_3H_3 successively hydrogenates to allene and propyne, couples to conjugated 2,4-hexadiyne, and dissociates to carbon deposits. An ample chemistry was exhibited in this unsaturated C_3H_3 ligand system.

2. Experimental and Computational Details

Experimental. The majority of the experiments were performed in an ultrahigh vacuum (UHV) chamber evacuated by a combination of ion and turbomolecular pumps. A base pressure below 1.0×10^{-10} torr was reached after baking. The chamber was equipped with an ion sputtering source for surface cleaning, a triple-filter quadrupole mass spectrometer for detecting residual gases as well as desorbing species from the surface, and RAIRS for collecting surface vibrational spectra. The Ag(111) single crystal (MaTeck, 99.999%) was attached to a heating element, mounted on a manipulator with capabilities for resistive heating to 1100 K and active cooling to 100 K by liquid nitrogen. A chromel−alumel thermocouple, whose junction was wedged into a hole in the side of the crystal, was used to measure the surface temperature. Programmed heating was achieved by a PID controller to ramp the temperature in a regulated fashion. TPD experiments were usually started by exposing the Ag(111) crystal to the sample vapors at 200 K, and the surface was then elevated to 950 K with a linear rate of 2 K/s. Upon being heated, multiple-ion signals and temperatures were collected synchronously. RAIRS was performed by taking the infrared beam from an FTIR spectrometer and focusing it at grazing incidence (85°) through a ZnSe wire-grid polarizer and a KBr window onto the Ag(111) in the UHV chamber. The reflected beam was then passed through a second KBr window and refocused on a liquid nitrogen-cooled HgCdTe detector. All spectra corresponded to the average of 512 scans at 4 cm^{-1} resolution and were ratioed against the background spectra from the clean metal surface. XPS were recorded in a separate UHV chamber connected to a wide-range (10−1500 eV) spherical grating monochromator beamline at the National Synchrotron Radiation Research Center in Hsinchu, Taiwan. Commercially available propargyl bromide (TCI, 97%), 1-propyn-1-yl iodide (TCI, 97%), and α,α-dimethyl-substituted propargyl chloride (3-chloro-3-methyl-1-butyne, Aldrich, 97%) were chosen as convenient precursors to generate $C_3H_{3(ad)}$ and its methyl-substituted version on Ag(111). Gas exposures were quoted as Langmuirs (L), uncorrected for ionization gauge sensitivity and collimator gain factor.

Computational. DFT calculations were carried out using the B3LYP functional as implemented in Gaussian 03. The computations were done using the LANL2DZ basis set. The Ag(111) surface was modeled by a single-layer Ag_{19} hexagonal cluster and a two-layer Ag_{22}(14, 8) cluster where 14 and 8 represent the numbers of the surface and the subsurface layer atoms, respectively. The clusters were fixed at a lattice constant of 2.889 Å. The hydrocarbon units were bound (not fixed) to the top Ag core atom with a trial Ag—C bond distance of 2.11 Å to start the calculations. All geometries were optimized fully without symmetry constraints. Frequency calculations were performed to confirm the nature of the stationary points and to obtain zero-point energies. Zero-point energy corrections were taken into account in obtaining the relative energies of intermediates and transition states. It was ensured that the calculated transition-state structures have one and only one imaginary vibrational frequency corresponding to the reaction coordinate. The frequencies given were corrected by a recom-

(2) Jemmis, E. D.; Chandrasekhar, J.; von Ragué Schleyer, P. *J. Am. Chem. Soc.* **1979**, *101*, 2848–2856.
(3) Reich, H. J.; Holladay, J. E. *J. Am. Chem. Soc.* **1995**, *117*, 8470–8471.
(4) Wojcicki, A. *Inorg. Chem. Commun.* **2002**, *5*, 82–97.
(5) Doherty, S.; Corrigan, J. F.; Carty, A. J.; Sappa, E. *Adv. Organomet. Chem.* **1995**, *37*, 39–129.
(6) Ogoshi, S.; Tsutsumi, K.; Ooi, M.; Kurosawa, H. *J. Am. Chem. Soc.* **1995**, *117*, 10415–10416.
(7) Vohs, J. M.; Barteau, M. A. *J. Phys. Chem.* **1987**, *91*, 4766–4776.
(8) Vohs, J. M.; Barteau, M. A. *J. Phys. Chem.* **1990**, *94*, 882–885.
(9) Vohs, J. M.; Carney, B. A.; Barteau, M. A. *J. Am. Chem. Soc.* **1985**, *107*, 7841–7848.
(10) Wu, Y.-J.; Wang, W.-H.; Chiang, C.-M. *Langmuir* **2002**, *18*, 1449–1452.
(11) Kung, H.; Lee, L.-C.; Wu, S.-M.; Cheng, H.-Y.; Chiang, C.-M. *J. Am. Chem. Soc.* **2007**, *129*, 1028–1029.

Scheme 1

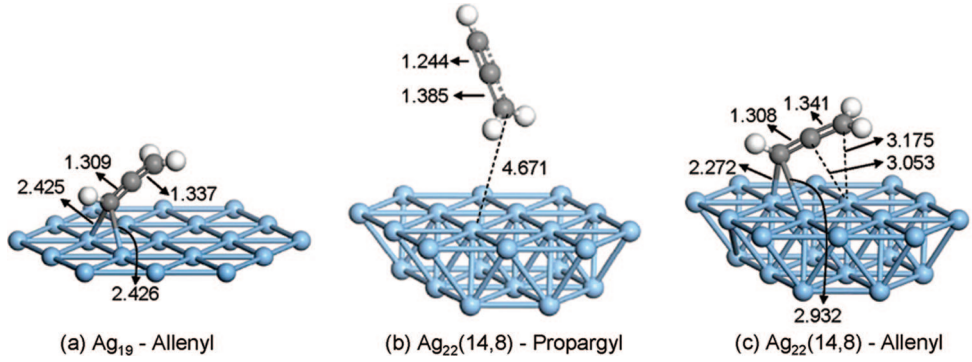

mended scaling factor of 0.9612 for systematic errors in this type of computation.[12]

3. Results and Interpretations

3.1. $C_3H_{3(ad)}$ Takes on η^1-Allenyl Form after C—Br Bond Cleavage of Propargyl Bromide at 200 K. The initial form of adsorbed C_3H_3 groups on Ag(111) was first investigated by performing RAIRS experiments with propargyl bromide Br—CH_2—C≡CH as the molecular precursor. Complementary DFT calculations were conducted to assist in determining the identity of the adsorbate, and animations of the normal modes allowed us to assign each frequency in the experimental IR spectra. Carbon−halogen bonds are relatively weak, and thus the desired hydrocarbon groups can be prepared by facile C—X (X = I, Br, and Cl) activation upon adsorption on metal surfaces.[13,14] In our previous X-ray photoemission study, the C—Br bond of adsorbed Br—CH_2—C≡CH on Ag(111) was found to break below 200 K.[10] In the same publication, owning to the limited signal-to-noise ratio of RAIRS, only two absorption features (1812 and 892 cm^{-1}) were visible in the spectra, but fortunately the 1812 cm^{-1} band was fairly diagnostic of a cumulenic C═C═C framework. In addition, there existed no sign for the terminal acetylenic ≡CH (>3200 cm^{-1}) and C≡C (>2000 cm^{-1}) vibrations, characteristics of the —CH_2—C≡CH unit. Thus the RAIR spectrum at 200 K implicated that the dominant surface species should be an *allenylic* Ag—CH═C═CH_2, rather than a propargylic Ag—CH_2—C≡CH. Here, this argument was strengthened by newer data after taking the RAIRS measurements to a wider spectral range and validated by theoretical calculations. The DFT calculation was launched with structure guessed as a "regular propargyl" unit bound to the Ag_{19} and Ag_{22}(14, 8) clusters. It is noteworthy that the optimized, energetically most stable ligand structures turn out to be a "bridged allenyl" unit on Ag_{19} (Scheme 1a) or a "twisted propargyl" species (CH_2 lies parallel with the CCC plane) distant from Ag_{22}(14, 8) with the closest Ag—C length being ∼4.7 Å (Scheme 1b). An additional DFT calculation was performed on "allenyl"—Ag_{22}(14, 8), which also renders a stable structure shown in Scheme 1c. Figure 1a−c exhibits the calculated IR frequencies built upon these resultant cluster-bound formalisms, and particularly those in Figure 1c appear to agree more reasonably with the absorption bands in Figure 1d, an experimental spectrum taken by exposing Ag(111) to 0.13 L (∼65% of monolayer saturation; see TPD in the next section) of propargyl bromide at 200 K. The peak at 1812 cm^{-1} correlates with the asymmetric C═C═C stretch. The peaks at 894 and 780 cm^{-1} represent α-C—H bending δ(C—H) and terminal CH_2 wagging ω(═CH_2) modes. The peaks predicted by theory but do not appear experimentally include ν(C—H), ν_s(═CH_2), and ν_s(C═C═C) stretches, which might be due to the detection limit of RAIRS sensitivity at a submonolayer coverage. Other vibrations, such as the ν_{as}(═CH_2 stretch), γ(CH_2 scissor), and ρ(═CH_2 rock), involve their oscillating dipole moments parallel to the surface and are IR-inactive on the basis of the surface dipole selection rule. Thus, the spectral differences between the experimental Figure 1d and the computational results Figure 1c are explicable.

Geometrically, the "allenyl" ligand binds to both the single- and two-layer metal frameworks (Scheme 1a,c) in a multinuclear fashion and perpendicularly bridges a Ag—Ag edge. Unlike that in Scheme 1a, the μ_2 structure in Scheme 1c, which allows a more satisfactory spectral match, is asymmetric with Ag—C contacts being 2.3 and 2.9 Å, respectively. The two CC bond lengths are 1.308 (internal) and 1.341 (external) Å, in line with an unperturbed C═C double bond distance.[4] The CCC skeleton is almost linear with a CCC angle of 174.8°. Therefore, π-interactions may be insignificant. Furthermore, because the two Ag—C distances from the middle carbon, as well as the terminal carbon to their nearest surface Ag atom are as far as

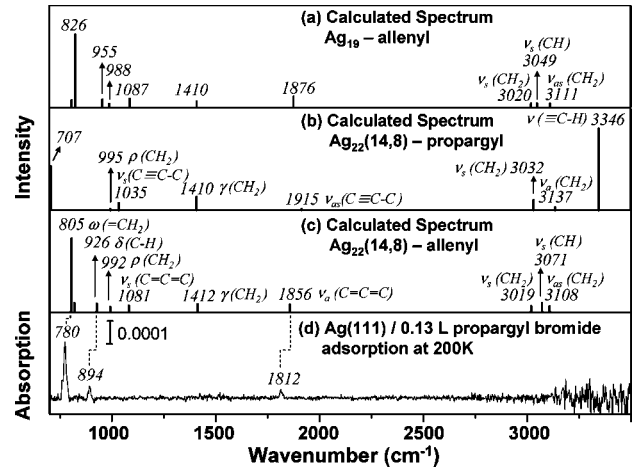

Figure 1. (a) IR spectrum based on the calculated structure of Scheme 1a. (b) Calculated spectrum based on the optimized structure of Scheme 1b. (c) Spectrum with normal mode assignments based on the calculated structure of Scheme 1c. (d) RAIR spectrum measured at 110 K following adsorption of a submonolayer coverage of propargyl bromide on Ag(111) at 200 K.

(12) National Institute of Standards and Technology. Computational Chemistry Comparison and Benchmark DataBase. http://cccbdb.nist.gov (accessed July 22, 2007).
(13) Zaera, F. *Chem. Rev.* **1995**, *95*, 2651–2693.
(14) Bent, B. E. *Chem. Rev.* **1996**, *96*, 1361–1390.

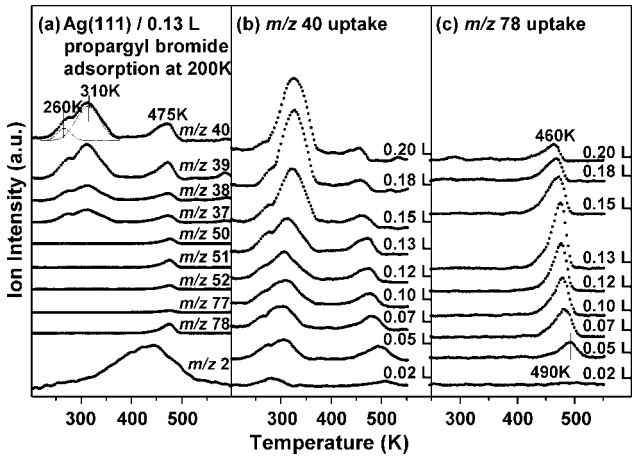

Figure 2. (a) Multiplex TPD spectra after adsorption of 0.13 L of $Br{-}CH_2{-}C{\equiv}CH$ on Ag(111) at 200 K. The broad feature of *m*/*z* 40 around 300 K is fitted with two Gaussian components (dotted curves). (b) The C_3H_4 (*m*/*z* 40) hydrogenation product yield as a function of propargyl bromide exposure. (c) The trend of *m*/*z* 78 signals that highlights change of C_6H_6 coupling product yield with increasing exposures.

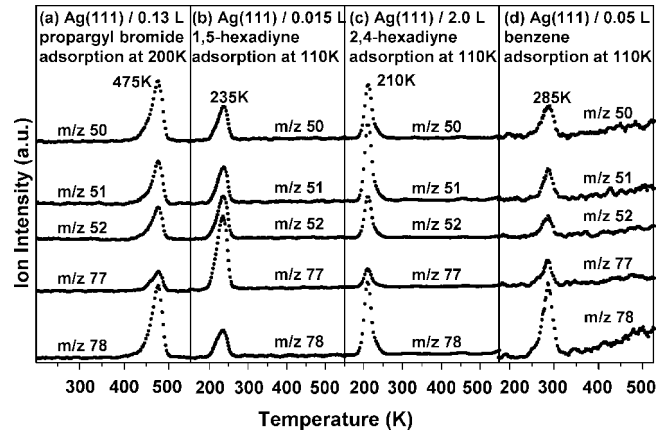

Figure 3. TPD spectra of representative ion fragments for C_6H_6 resulting from adsorption of (a) $Br{-}CH_2{-}C{\equiv}CH$, (b) $HC{\equiv}CCH_2{-}CH_2C{\equiv}CH$, (c) $CH_3C{\equiv}C{-}C{\equiv}CCH_3$, and (d) benzene on Ag(111).

3.053 and 3.175 Å, multidentate configurations such as metallacycles may be tentatively ruled out.

3.2. Three-Phase Self-Hydrogenation of $C_3H_{3(ad)}$ on Silver (260, 310, and 475 K). Silver surfaces are unique in their ability (or selectivity) to couple hydrocarbon species without inducing dehydrogenation and hydrogenation reactions, which has been addressed in several recent review articles.[14,15] Surprisingly, multiplex TPD results after dosing 0.13 L of propargyl bromide on Ag(111) at 200 K show hydrogenation products (C_3H_4) evidenced by the signals from *m*/*z* 40($C_3H_4^+$), 39($C_3H_3^+$), 38($C_3H_2^+$), and 37(C_3H^+) in Figure 2a. Allene and propyne are both qualified C_3H_4 species but have essentially the same cracking pattern in mass spectrometry, making their discrimination in TPD problematic. The broad desorption profiles around 300 K led us to consider that more than one species is present around this temperature, and two components, with peak maxima at 260 K (shoulder) and 310 K, can be resolved by a curve-fitting analysis imposed on the *m*/*z* 40 signals (dotted lines). Figure 2b illustrates the change of C_3H_4 yields with increasing exposures, and clearly saturation is reached at about 0.2 L. At 475 K, a coupling product, namely a C_6H_6 dimer, is indicated by a set of concurrent *m*/*z* 78($C_6H_6^+$), 77($C_6H_5^+$), 52($C_4H_4^+$), 51($C_4H_3^+$), and 50($C_4H_2^+$) ion signals in Figure 2a. Because fragmentation of C_6H_6 in a mass spectrometer contributes insignificantly to *m*/*z* 40($C_3H_4^+$), an additional desorption state of the hydrogenation product C_3H_4 occurs at this temperature as well. Other mass fragments such as *m*/*z* 42($C_3H_6^+$) and 44($C_3H_8^+$) were not detected; therefore, hydrogenation to more highly saturated hydrocarbons does not take place. Different from active transition metals, the dissociation of the background H_2 should be inefficient on a silver surface under vacuum, because of a large barrier to the formation of chemisorbed H atoms, thus suggesting that the surface C_3H_3 moieties undergo self-hydrogenation (hydrogen from dissociated $C_3H_{3(ad)}$) to C_3H_4. In fact, a very broad hydrogen evolution profile (*m*/*z* 2) spanning from 300 to 500 K is detected, indicating progressive thermal alteration of the surface H/C ratio. A coexisting polymeric hydrocarbonaceous deposit, presumably composed of fragments such as CH_2, CH, or C_2H, might be developed upon the sequential dehydrogenation of the original $C_3H_{3(ad)}$ (see section 3.4 for C 1s XPS). It is likely that this type of active carbon species serves as the hydrogen reservoir.

3.3. C—C Coupling Product Is 2,4-Hexadiyne rather than 1,5-Hexadiyne. Candidates for the C_6H_6 coupling end product emcompass isomers such as benzene, 1,5-hexadiyne, or 2,4-hexadiyne. According to the NIST standard mass spectra,[16] 2,4-hexadiyne accounts best for the liberated C_6H_6 at 475 K resulting from the propargyl bromide. To substantiate this identification, 1,5-hexadiyne, 2,4-hexadiyne, and benzene were individually physisorbed on Ag(111) at 110 K and diagnosed by our mass spectrometer upon subsequent thermal desorption. The *m*/*z* 50, 51, 52, 77, and 78 TPD data from propargyl bromide, 1,5-hexadiyne, 2,4-hexadiyne, and benzene are juxtaposed in Figure 3a—d, respectively. On the basis of these fragments' relative intensity patterns, it should be safe to declare that the desorbing species at 475 K is surely 2,4-hexadiyne. Moreover, the difference of the TPD peak maxima (475 vs 210 K) indicates that the rate of C_6H_6 formation pathway is not limited by the final desorption step. Second-order kinetics is implied by a TPD peak shift toward lower temperatures from 0.05- to 0.13-L exposures, as shown in Figure 2c. The yield of the C_6H_6 TPD feature maximizes by 0.13 L and diminishes afterward, implying that the dimerization step is suppressed, perhaps due to inhibited surface diffusion at higher coverages of adsorbates and carbon deposits. The discovery of a C—C coupling product is not unexpected and seems to add another example for this type of reactivity on silver surfaces, in addition to the couplings of alkyls,[17] vinyl,[17,18] phenyl,[18] allyl,[19,20] and 1-propynyl (methylacetylide) intermediates.[11]

In this vein, with chemisorbed propargyl bromide as the starting molecule, surface-catalyzed C—C homocoupling reaction is foreseen to give rise to bispropargyl (1,5-hexadiyne). The rendering of 2,4-hexadiyne in TPD, however, makes us wonder if this C_6 end product actually stems from *dimerization of methylacetylide* ($Ag{-}C{\equiv}C{-}CH_3$) which certainly should not

(15) Ma, Z.; Zaera, F. *Surf. Sci. Rep.* **2006**, *61*, 229–281.
(16) National Institute of Standards and Technology. NIST Chemistry WebBook, NIST Standard Reference Database Number 69, June 2005 Release. http://webbook.nist.gov/chemistry (accessed November 25, 2007).
(17) Zhou, X.-L.; White, J. M. *J. Phys. Chem.* **1991**, *95*, 5575–5580.
(18) Zhou, X.-L.; Schwaner, A. L.; White, J. M. *J. Am. Chem. Soc.* **1993**, *115*, 4309–4317.
(19) Carter, R. N.; Anton, A. B. *J. Am. Chem. Soc.* **1992**, *114*, 4410–4411.
(20) Celio, H.; White, J. M. *J. Phys. Chem. B* **2001**, *105*, 3908–3916.

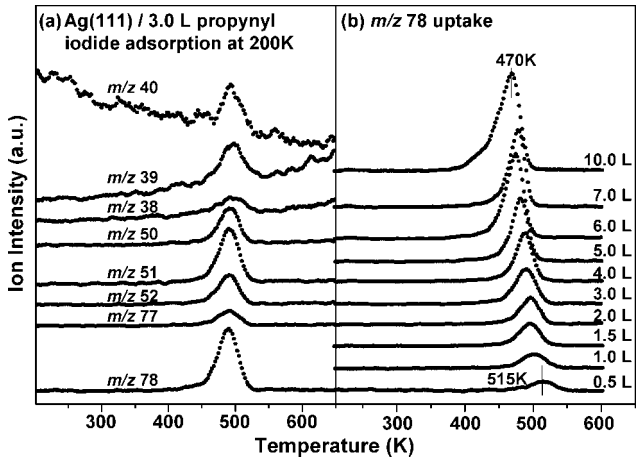

Figure 4. (a) Multiplex TPD spectra after adsorption of 3.0 L of $I-C\equiv CCH_3$ on Ag(111) at 200 K. (b) The trend of *m*/*z* 78 signals which highlights change of the homocoupling product (2,4-hexadiyne) yield with increasing exposures. Saturation is reached at about 6.0 L.

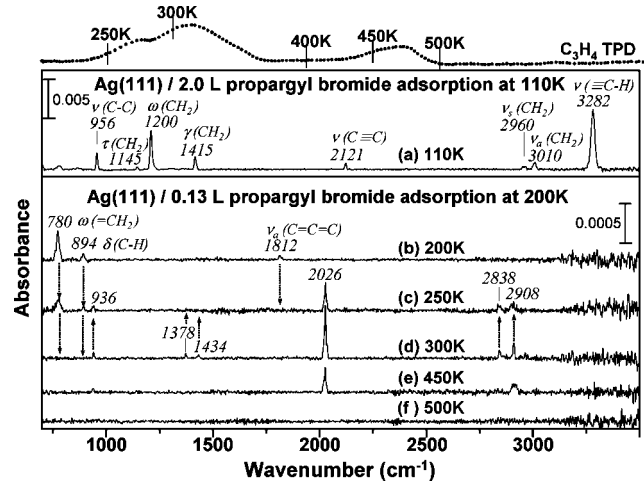

Figure 5. RAIR spectra of (a) 2.0 L of $Br-CH_2C\equiv CH$ physisorbed at 110 K, sufficient to populate the multilayer on Ag(111) and (b) 0.13 L of propargyl bromide adsorbed at 200 K (~65% of monolayer saturation). Spectra c−f were measured at 110 K following momentary annealing of sample (b) to the temperatures indicated. TPD trace of the hydrogenation product C_3H_4 is on top as a guide to the thermal pathway.

be forgotten as a feasible surface-bound C_3H_3 isomer. In other words, appearance of this internally conjugated diyne alludes to the likelihood that multiple propargyl−allenyl−acetylide isomerization is operational. Concrete evidence for the presence of a methylacetylide species can be established by TPD study using adsorbed 1-propyn-1-yl iodide ($I-C\equiv C-CH_3$) as a direct route to $Ag-C\equiv C-CH_3$. Figure 4a shows that, following adsorption and C−I bond scission of 3.0 L (~50% of monolayer saturation) of $I-C\equiv C-CH_3$ at 200 K, methylacetylides on Ag(111) are thermally stable at least to 400 K and then indeed afford $CH_3-C\equiv C-C\equiv C-CH_3$ (*m*/*z* 78, 77, 52, 51, 50) as well as C_3H_4 (*m*/*z* 40, 39, 38) around 500 K. Here, the chemistry undertaken around 500 K is qualitatively the same, but, contrary to the TPD results from the propargyl bromide initiation, the relative abundance of *m*/*z* 78 vs 40 at 500 K (compare Figure 4a with Figure 2a) reveals that the C_6 coupling product now becomes the preferential desorbing species from direct methylacetylide initiation (no pre-existent carbonaceous species on the surface). Moreover, the uptake of C_6H_6 yields as a function of exposure exhibits a saturation behavior, instead of passing through a maximum, as shown in Figure 4b vs Figure 2c.

3.4. η^1-Allenyl to η^1-Methylacetylide Transition (250−300 K): [1,3]-Hydrogen Shift. Temperature-dependent RAIRS and XPS measurements were conducted to substantiate the hinted allenyl−methylacetylide conversion from TPD. Figure 5a exhibits the condensed multilayer RAIR spectrum after exposing Ag(111) to 2.0 L of $Br-CH_2-C\equiv CH$ at 110 K. Eight major absorption bands and their vibration mode assignments, 956 cm^{-1} ν(C−C stretch), 1145 cm^{-1} τ(CH_2 twist), 1200 cm^{-1} ω(CH_2 wag), 1415 cm^{-1} γ(CH_2 scissor), 2121 cm^{-1} ν(C≡C stretch), 2960 cm^{-1} ν_s(CH_2 stretch), 3010 cm^{-1} ν_a(CH_2 stretch), and 3282 cm^{-1} ν(≡C−H stretch), match well those of the gas-phase compound.[21] A series of RAIR spectra, shown in Figure 5b−f, were obtained by dosing 0.13 L of propargyl bromide (~65% of monolayer saturation) at 200 K and subsequent annealing to several key temperatures directed by the *m*/*z* 40 TPD curve. Figure 5b is equivalent to Figure 1b and is just a reminder that the three observable bands, 780, 894, and 1812 cm^{-1}, were utilized to argue for the Ag-η^1-allenyl form in section 3.1. After momentary annealing to 250 K, a number of new bands emerge from 936, 2026, 2838, and 2908 cm^{-1} in Figure 5c; however, two of the signals diagnostic of η^1-allenyl (780 and 894 cm^{-1}) still persist. This spectral development suggests that allenyl begins to transform upon heating to generate an equilibrium mixture of η^1-allenyl and a new surface species. The 300 K annealing ultimately makes the 780 and 894 cm^{-1} features disappear; instead, two more new bands (1378 and 1434 cm^{-1}) arise, as shown in Figure 5d. The rest of the vibration features grow stronger. Finally, synchronous with the onset of C_3H_4 and C_6H_6 liberation in TPD, the weaker bands in Figure 5e start to diminish or even vanish. Entire infrared signals eventually fade out above 500 K.

At the critical juncture (250−300 K), what is happening on the surface relies on the answer to why the fingerprinting C=C=C stretch mode (1812 cm^{-1}) is superseded by a C≡C stretch mode (2026 cm^{-1}). A previous proposal[10] suggested that such a dramatic spectral variation correlates with molecular transformation from allenyl ($Ag-CH=C=CH_2$) back to propargyl ($Ag-CH_2-C\equiv CH$) formalism in $Ag-C_3H_3$ (i.e., tautomerization). Yet in view of the supporting RAIRS data (Figure 6) acquired independently from the third alternative intermediate, namely $Ag-C\equiv C-CH_3$ (methylacetylide), that proposal needs to be revised here.

It turns out that the six characteristic bands in Figure 5d agree remarkably well with those in the spectrum of Figure 6c, gained by exposing Ag(111) to 3.0 L of $I-C\equiv C-CH_3$ at 200 K. The theoretical IR spectra, built upon the optimized structure for methylacetylide bonded to the Ag_{19} and $Ag_{22}(14,8)$ clusters (Scheme 2a,b) by DFT calculations, are also displayed in Figure 6a,b with vibration-mode designations. On the basis of the animated normal vibrations in the theoretical modeling, it should be noted that those pronounced peaks in the experimental Figure 5b and Figure 6c at 2904, 2042, 1367, and 944 cm^{-1}, corresponding to $\nu_s(CH_3)$, ν(C≡C), $\delta_s(CH_3$ deformation), and ν(C−C) modes, are all associated with their dynamic dipole moments parallel to the CCC axis, implying that the methylacetylide moiety adopts a stand-up geometry on the surface, conformable to the DFT results which predict unanimously in both single- and two-layer models that the C_3H_3 ligand coordinates to the surface via a rare μ_3-η^1-bonding mode at a location near the 3-fold hollow site instead of a conventional

(21) Shimanouchi, T. *J. Phys. Chem. Ref. Data* **1977**, *6*, 993–1102.

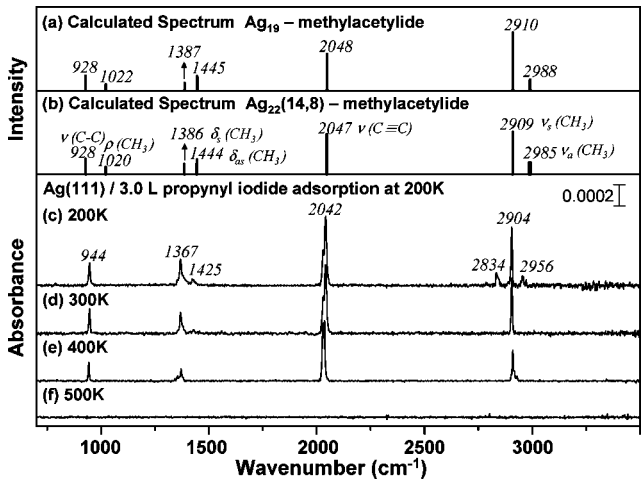

Figure 6. (a) Theoretically predicted IR spectrum for C≡CCH_3 unit bound to a Ag_{19} cluster. (b) Calculated spectrum with mode assignments based on the animated vibrations of the optimized structure for the C≡CCH_3 unit bound to a Ag_{22}(14,8) cluster. (c) Experimental RAIR spectrum collected after a 3.0-L exposure of the Ag(111) surface at 200 K to I—C≡CCH_3 (~50% of monolayer saturation). Spectra d–f were measured following annealing of sample (c) to the temperatures indicated.

Scheme 2

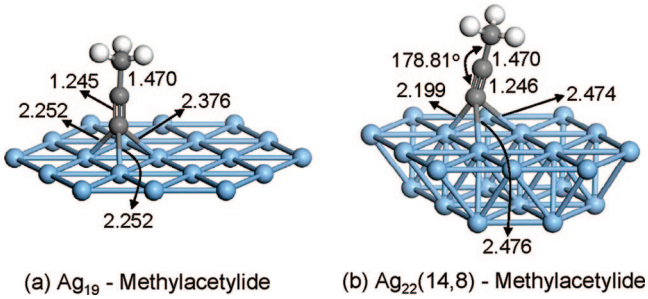

terminal atop position (see the Discussion). In the perhaps more realistic Ag_{22}(14,8) calculations, the silver–acetylide triple bridge is markedly asymmetric, with the respective Ag—C bond lengths being 2.199, 2.474, and 2.476 Å. Also, the CCC axis is not entirely upright and the tilt angle is ~16° relative to the surface normal as shown in Scheme 2b; therefore a "side-on" π-bonding is deemed possible. However, the small deviation from linearity of the —C≡CCH_3 unit ($\angle$CCC = 178.8°) and the absence of frequency shift regarding the C≡C stretch (cf. 2038 cm^{-1} of bulk I—C≡CCH_3 in KBr[11]) reflect negligible η^2- or η^3-type interactions (pure σ-type bonding). Above 300 K, the rest of the spectra in Figure 6d–f also faithfully mirrors the trends in Figure 5. When the information (TPD, RAIRS, and DFT) is taken together, we feel confident that Ag—C≡C—CH_3 (methylacetylide) must engage in the intramolecular transformation process.

Allenyl–methylacetylide conversion, in lieu of allenyl–propargyl tautomerization, is corroborated by XPS taken in a separate UHV chamber at the Taiwan synchrotron facilities. Here, the reported exposures of the XPS data were set at the product saturation coverages calibrated by TPD in that vacuum system. In Figure 7a, the C 1s photoemission spectrum following adsorption of propargyl bromide on Ag(111) at 200 K exhibits a broad and asymmetric feature at binding energy (BE) 283.7 eV with a full width at half-maximum (fwhm) of 1.27 eV. We make no attempt here to resolve the three different chemical environments of carbon atoms in the molecule because neither

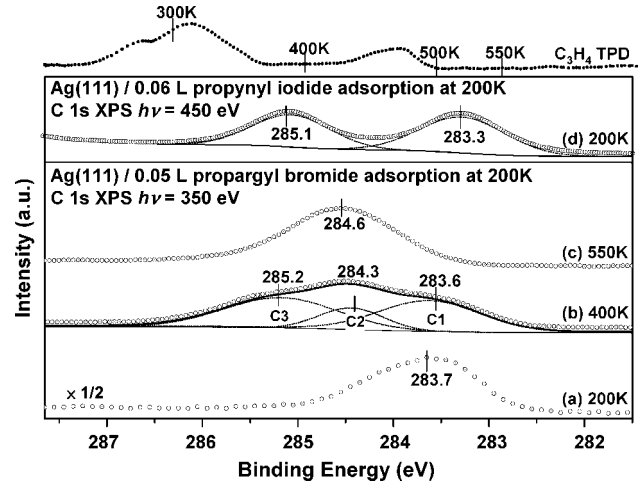

Figure 7. C 1s XPS measured after (a) exposing Ag(111) to Br—CH_2C≡CH at 200 K and (b) annealing sample (a) to 400 K. Here, scattered points and solid lines are experimental raw data and fitted curve. The dotted lines show three possible components. For peak labeling, C1, along with C3, is indicative of methylacetylide, and C2 is a sign of carbonaceous species. (c) Spectrum after annealing sample (a) to 500 K. (d) Separate measurement after exposing Ag(111) to I—C≡CCH_3 at 200 K. The spectrum can be resolved into two peaks portrayed by the dotted lines.

the chemisorbed nor gas-phase literature BE values for the allenyl species are available. After the surface is annealed to 400 K where the first two types of self-hydrogenation products (referring to the TPD trace on top of Figure 7) have completed their evolution, the C 1s spectrum shows notable changes in Figure 7b. First, the overall feature becomes extremely wide and shifts toward higher BEs. Deconvolution analysis, in which Shirley baseline is applied and line shapes are fitted with 100% Gaussian, reveals that this spectrum is best fitted with three components, shown as the dotted lines with peak maxima at 283.6 (C1), 284.3 (C2), and 285.2 eV (C3), respectively. Second, the integrated peak intensity is attenuated by about 28% with respect to spectrum (a). A previous XPS study of adsorbed methylacetylide formed by the reaction of propyne with O(ad) on Ag(110) showed only two C 1s peaks in a 5:3 ratio centered at 283.1 and 284.9 eV.[9] To be certain, we carried out separate XPS measurements for methylacetylide by dissociatively adsorbed 1-propyn-1-yl iodide (I—C≡C—CH_3) at 200 K on Ag(111). The C 1s spectrum (Figure 7d) also illustrates two peaks in a 5:4 ratio centered at 283.3 and 285.1 eV, qualitatively similar to Barteau et al.'s findings.[9] The discrepancies might be due to the electronic effects originating from the utilization of halide compounds as the $C_3H_{3(ad)}$ precursors in our case. Yet the comparable BE information of Figure 7d ensures assignments of the C1 and C3 peaks to methylacetylides in Figure 7b. The remaining C2 peak at 284.3 eV can be carbon-bonded to hydrogen (CH_x),[22] confirming that the surface may be partially covered with a carbonaceous (or hydrocarbonaceous) overlayer. It is quite possible that hydrogen transfer to the $C_3H_{3(ad)}$ may be mediated by this type of active carbon deposits,[23] rather than via direct addition of adsorbed hydrogen atoms on the bare silver sites (Ag has low affinity for hydrogen[24]). Finally, when the surface containing methylacetylide is heated to 550 K, only a

(22) Moussaif, N.; Pagnoulle, C.; Riga, J.; Jérôme, R. *Polymer* **2000**, *41*, 3391–3394.
(23) Somorjai, G. A.; Zaera, F. *J. Phys. Chem.* **1982**, *86*, 3070–3078.
(24) Healey, F.; Carter, R. N.; Hodgson, A. *Surf. Sci.* **1995**, *328*, 67–79.

single C 1s peak with BE at 284.6 eV (graphitic) is observed in Figure 7c. The ratio of the peak area to that in Figure 7a is found to be ~57%. We reason that above 500 K the carbonaceous deposits from sequential hydrocarbon dissociations eventually lose all the hydrogen content in the process of hydrogenation as well as H_2 evolution (see the broad TPD feature in Figure 2a), and enough thermal energy is present for the carbon species left on the surface to coalesce into passive graphitic residues.

Nominally, to convert Ag−CH═C═CH_2 into Ag−C≡C−CH_3 simply requires hydrogen migration to the new location with a reorganization of the π-bonds, maintaining the total number of σ-bonds and π-bonds unchanged. However, such a thermal [1,3]-hydrogen shift especially with its rate facility (only 250 K) is not entirely indisputable because the process involves the relocation of two pairs of bonding electrons (one σ-bond and one π-bond) and is thus symmetry forbidden suprafacially.[25] Under thermal conditions, the situation can be made feasible by proceeding via a Möbius transition state where the hydrogen, initially σ-bonded with one face of the π-unit, ends up connecting the bond at the opposite face of the terminus, namely an antarafacial [1,3]-shift. It is remarkably difficult to design a practical experiment to differentiate between the supra and antara routes. To lift the Woodward−Hoffmann restriction as well as to avoid a strained antarafacial transition state, it is possible that a multistep pathway, with the involvement of the metal surface and/or the coadsorbed halogen, is responsible for the revealed low activation barrier.

3.5. Methyl Substitution Suggests that Incipient Propargyl to Allenyl Transformation Is via [1,3]-Sigmatropic Rearrangement. In section 3.1, RAIRS and DFT calculations concluded that Ag−C_3H_3 favors the η^1-Ag−CH═C═CH_2 presentation subsequent to the initial dissociative adsorption of Br−CH_2−C≡CH at 200 K. Likewise, this metal-bonded "allenyl" can be envisioned to alter from the bromine-bonded "propargyl" via a [1,3]-hydrogen shift. Thus, the net reaction can be described as Br−*CH_2C≡CH → Ag−*CH═C═CH_2 with retention of the same labeled carbon σ-bonded to metal. However, the second plausible scenario is that the C_3H_3 skeletal reorganization actually involves a [1,3]-sigmatropic rearrangement, in which the σ-bond migrates over the hydrocarbon framework to cause a change in the locus of metal−ligand bonding (i.e., Br−*CH_2C≡CH → *CH_2═C═CH−Ag).

A propargylic reagent with methyl substituents, such as Cl−$(CH_3)_2$*CC≡CH without hydrogen available at the labeled carbon, would rule out the pathway for the [1,3]-hydrogen shift. The only possible η^1-allenyl formed (if any) after breaking the C−Cl bond (bromide compound is not available) would solely be $(CH_3)_2$*C═C═CH−Ag through a shift of the σ-bond from one terminal carbon to the other. Figure 8b−d shows RAIR spectra measured by dosing 0.1 L of Cl−$(CH_3)_2$CC≡CH at 200 K and followed by annealing to the specified temperatures. In the spectrum of Figure 8b, the fingerprinting allenic ν_{as}(C═C═C) mode around 1900 cm^{-1} is invisible. Major absorption features include 1011, 1292, 1375, 1443 cm^{-1}, and several bands above 2800 cm^{-1}. DFT calculations were performed by starting with a dimethyl-substituted "allenyl" format bearing the two methyl groups at the terminal position as the trial structure on the Ag_{22}(14,8) cluster, and the preferred structure is shown in Scheme 3. The computed spectrum for

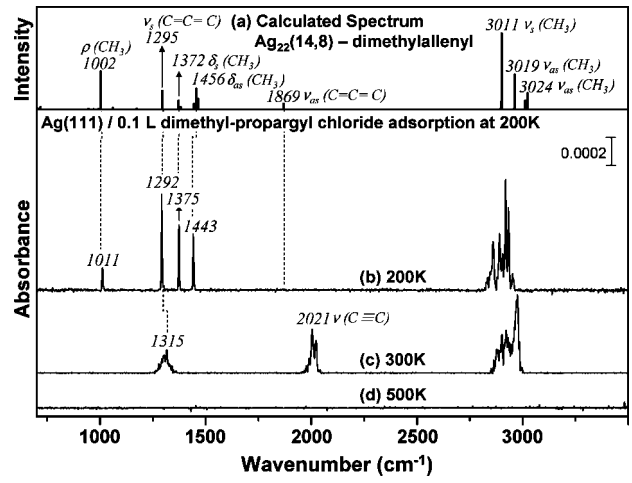

Figure 8. (a) Theoretically predicted IR spectrum with mode assignments based on the animated vibrations of the calculated structure for the −CH═C═$C(CH_3)_2$ unit bound to a Ag_{22}(14,8) cluster shown in Scheme 3. (b) Experimental RAIR spectrum collected after a 0.1-L exposure of Ag(111) surface at 200 K to Cl−$(CH_3)_2$CC≡CH. Spectra (c) and (d) were measured following annealing of sample (b) to the temperatures indicated. Above 500 K, all spectral features disappear.

Scheme 3

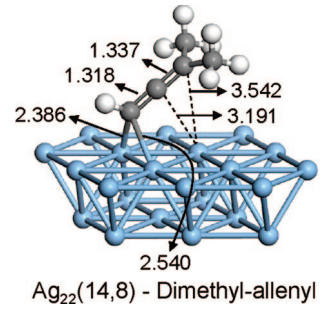

this structure (Figure 8a) resembles that derived from the chemisorption experiments in Figure 8b. Particularly, the prominent 1292 cm^{-1} band can be assigned to the allenic symmetric stretch ν_s(C═C═C) mode; yet the less intense asymmetric C═C═C stretch predicted by theory becomes invisible experimentally. The C−H stretches from the *terminal* CH_3 groups, and the α-C−H are absorption bands in the 2800−3000 cm^{-1} range. The peaks at 1375 and 1443 cm^{-1} are ascribed to the CH_3 symmetric and asymmetric deformation modes, respectively. The remaining one at 1011 cm^{-1} is attributable to the $\rho(CH_3$ rock). Such fair agreements ratify that the primary propargyl-to-allenyl conversion should consist of facile carbon−halogen bond cleavage and a much smoother [1,3]-sigmatropic rearrangement, rather than [1,3]-hydrogen transfer, at 200 K. However, the concerted nature, namely, a detailed η^1-η^3-η^1 movement or slippage of the CCC unit is not directly seen because of a lack of spectroscopic evidence for the η^3-intermediacy.

From 200 to 300 K, the most notable change is the advent of new bands at 2021 cm^{-1} (as a doublet in Figure 8c). The collateral rise of the 2021 cm^{-1} and fall of the 1292 cm^{-1} around the analogous temperatures are reminiscent of the switch from allenic C═C═C to alkynic C≡C functionality found in the normal C_3H_3 species. This observation serves as another testimony for the secondary conversion where hydrogen now needs to relocate, ushering Ag−CH═C═$C(CH_3)_2$ into Ag−C≡C−$CH(CH_3)_2$.

(25) Lowry, T. H.; Richardson, K. S. *Mechanism and Theory in Organic Chemistry*, 3rd ed.; HarperCollins: New York, 1987; pp 944−971.

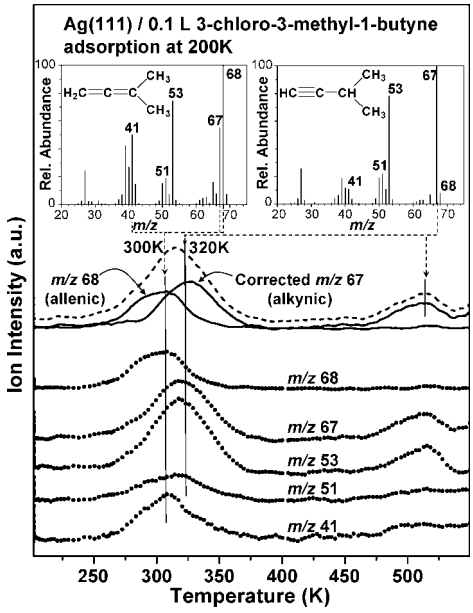

Figure 9. Multiplex TPD after dosing 0.1 L of Cl—$(CH_3)_2$C—C≡CH on Ag(111) at 200 K. Scattered points are raw TPD data for various ions. The dashed line is obtained by a combination of the *m*/*z* 68 and the corrected *m*/*z* 67 (see the text for the correction) data (solid lines), respectively. Insets are standard fragmentation patterns of 3-methyl-1,2-butadiene and 3-methyl-1-butyne excerpted from the NIST database.[16]

3.6. Methyl-Substituted Propargylic Species Lend Support to Verification of the Identity for Each Hydrogenation Product. In section 3.2, TPD spectra disclosed three individual C_3H_4 evolution states with peak maxima at 260, 310, and 475 K, originating from $C_3H_{3(ad)}$ self-hydrogenation. We were confronted by a predicament that the identification of allene and propyne via mass spectrometry is not definitive. The use of dimethyl-substituted propargyl chloride, Cl—$(CH_3)_2$C—C≡CH, has also assisted in working around this limitation. Unlike the difficult situation of allene vs propyne, the fragmentation patterns of $(CH_3)_2$C=C=CH_2 and $(CH_3)_2$CH—C≡CH, resulting from self-hydrogenation of the dissociatively adsorbed Cl—$(CH_3)_2$C—C≡CH, become discernible. The relative intensity of *m*/*z* 67 ($C_5H_7^+$, "M − 1" ion) to *m*/*z* 68 ($C_5H_8^+$, "M" parent ion) is fairly distinctive for the two species, referring to the NIST mass spectra shown in the inset of Figure 9. In particular, $(CH_3)_2$CH—C≡CH has a very minor fragment of *m*/*z* 68 (only ~8% relative to *m*/*z* 67, which is the most abundant ion). In sharp contrast, *m*/*z* 68 is the most abundant ion for $(CH_3)_2$C=C=CH_2. Figure 9 shows the TPD spectra obtained after dosing 0.1 L of Cl—$(CH_3)_2{}^{\alpha}$C—C≡C—H on Ag(111) at 200 K. First, the desorption feature at 500 K, characterized by *m*/*z* 67, 53, however, almost devoid of 68, strongly suggests that the alkynic $(CH_3)_2$CH—C≡CH is the hydrogenation product at this temperature. Second, the interpretations for the desorption profiles between 250 and 350 K are more subtle, and we need to think of them as a mixture of two species, consisting of allenic $(CH_3)_2$C=C=CH_2 with its peak position at 300 K diagnosed by the *m*/*z* 68 signals and alkynic $(CH_3)_2$CH—C≡CH with peak position at 320 K represented by *m*/*z* 67 signals. Also, the desorption maximum of *m*/*z* 41 (the fourth largest fragment for the allenic species but quite insignificant for the alkynic isomer) inclines toward 300 K, which lends support to the above products recognition. Furthermore, we deliberately take 55% of the *m*/*z* 68 counts (i.e., the allenic part contribution to the *m*/*z* 67) and subtract that out of the total *m*/*z* 67 TPD signals.

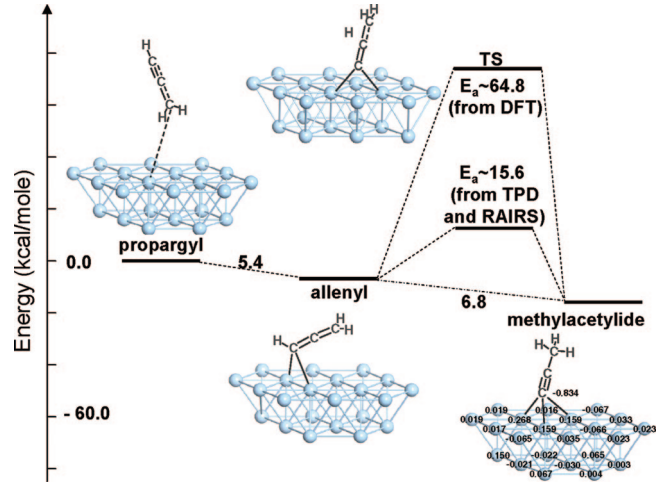

Figure 10. Energy diagram for the three possible C_3H_3 intermediates on a Ag(111) surface. The thermodynamic stability data are based on DFT calculations, including zero-point corrections. The kinetic information about the barrier heights for the allenyl-to-acetylide rearrangement is estimated from the experimental RAIRS and TPD data as well as DFT computation. Calculated charges by natural population analysis (NPA) are labeled for Ag_{22}(18,4)—C≡CCH_3 to reveal the electrostatic ligand-cluster bonding nature.

This corrected *m*/*z* 67 (standing for pure alkyne) curve when overlapped with the *m*/*z* 68 data (almost pure allene) constitutes an envelope (i.e., the dashed line in Figure 9), which provides an insight into the convoluted *m*/*z* 40 TPD trace in the case of normal propargyl bromide (Figure 2a). Although the above analysis might not be rigorously quantitative, it is valid for resolving and identifying the hydrogenation products qualitatively.

To account for the sequence of 260 K allene and ensuing 310 K propyne formation, a portion of the initial propargyl/allenyl species (after C—Br bond scission) must be thermally unstable on silver surfaces, consistent with Barteau et al.'s conclusion on Ag(110),[9] and decompose rapidly to a carbonaceous layer, thus furnishing the Ag—$^{\alpha}$CH=C=CH_2 and the next generated Ag—$^{\alpha}$C≡CCH_3 (beginning at 250 K) with hydrogen atoms to reductively eliminate allene at 260 K and propyne at 310 K (single hydrogen incorporation to the α-carbon). However, hydrogen transfer might only take place at the peripheries of the carbonaceous island interpreted by the fractional desorption kinetics in C_3H_4 TPD spectra in Figure 2b (referring to the increasing peak temperature toward higher coverages), while the H atoms within the carbon clusters are always liberated in the form of H_2. It is thus less efficient to make all the strongly binded surface methylacetylide moieties move to the edges and be hydrogenated. The survived Ag—C≡CCH_3 needs to wait for its own dissociation above 400 K to accomplish the final self-hydrogenation in conjunction with the C—C homocoupling.

3.7. Proposed Mechanism and Energy Diagram. The RAIRS, TPD, XPS, and DFT characterization of the chemistry for unsaturated C_3H_3 groups on Ag(111) can be united to develop a fairly detailed picture of the steps involved in the surface propargyl—allenyl—methylacetylide evolution. A summary of our proposed mechanism is provided in Scheme 4.

It should be mentioned that the C—C σ-bond formation is the most favored step on silver surfaces. The reaction temperature for allenyl—allenyl homocoupling, creating a $C_{sp}{}^2$—$C_{sp}{}^2$ bond, should be close to that for the vinyl—vinyl coupling, which was found to be at 260 K on Ag(111).[17,18]

Scheme 4

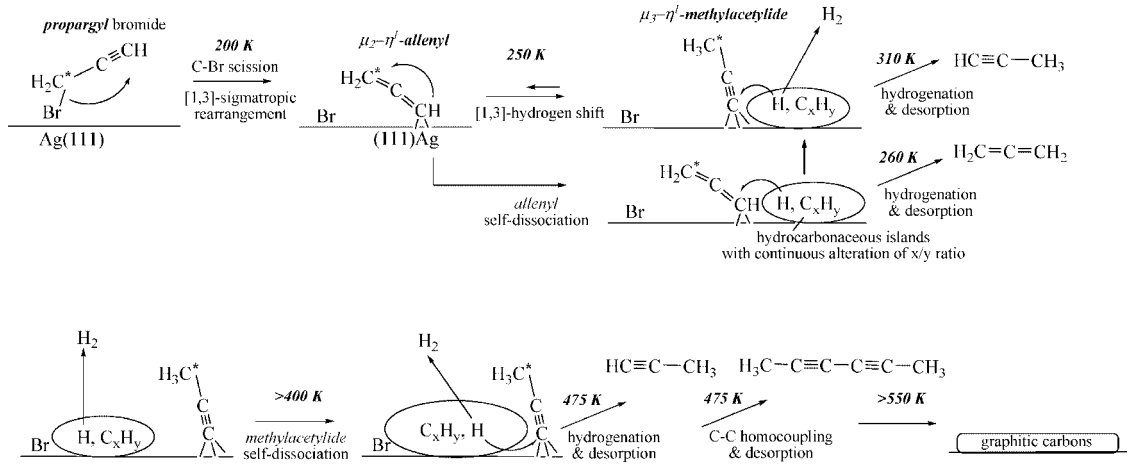

This is slightly higher than the temperature for the allenyl−methylacetylide transition (250 K); therefore, a low-temperature coupling route is undetected because isomerization ([1,3]-hydrogen shift) can compete favorably with the $C_{sp}{}^2$—$C_{sp}{}^2$ coupling. However, the methylacetylide−methylacetylide homocoupling, making a C_{sp}—C_{sp} connection, obviously takes place above 450 K to afford 2,4-hexadiyne. Regardless of the stronger metal−carbon (sp-hybridized) bond as well as the anionic character of the metal acetylide species,[11] the access to this high-temperature coupling channel might be related to the codeposited halogens which alter the electronic structure of the surface Ag atoms. The halogen modification is also known to make the Ag surfaces become open to the dehydrogenation reactions for chemisorbed hydrocarbon fragments.[26]

Energetically speaking, the first $-CH_2-C\equiv CH \rightarrow CH_2=C=CH-$ conversion might be driven by the tendency toward equalizing bond distances for better σ-orbital overlapping under a more symmetric CCC framework.[27] The second $CH_2=C=CH-Ag \rightarrow CH_3-C\equiv C-Ag$ internal rearrangement might be due to a demand for the surface-bound carbon to turn sp-hybridized (electrons in a high s-character orbital benefit from closer proximity to the nucleus), which is more advantageous to the electrostatic interactions between the possibly negatively charged $CH_3-C\equiv C^{-\delta}$ and the surface metal atoms. The M—C bond strengths generally follow the order of $sp^3 < sp^2 < sp$,[28] and the course of the propargyl−allenyl−methyacetylide bond reorganization coincides with the increasing s-character in the hybridized α-carbon orbital. The thermodynamically favorable order of appearance for these various intermediate states properly reflects the stepwise migration of the triple bond from the terminal to the internal position.

By using the less complicated LANL2DZ basis set and the practical two-layer fixed $Ag_{22}(18,4)$ cluster model, the predicted vibration frequencies agree well with those observed experimentally, granting us the confidence to analyze the relative energy profile of the surface intermediates. In Figure 10, we summarize the DFT calculated energy diagram for the Ag_{22}—C_3H_3 system. The anticipated relative stability of propargyl, allenyl, and methylacetylide, along with a trend toward multisite coordination (binuclear−trinuclear), is manifested. Kinetically speaking, the conversion from propargyl bromide to allenyl is instantaneous at 200 K, but the exact propargyl-to-allenyl transition remains implicit. The actual proceeding of allenyl to methylacetylide via [1,3]-hydrogen transfer occurs at 250 K according to surface IR; however, TPD can only detect the resulting propyne (hydrogenation of the methylacetylide) at 310 K. The former temperature is utilized to obtain an activation energy of ~15.6 kcal/mol using Redhead's first-order analysis with a 10^{13} s^{-1} prefactor and a heating rate of 2 K/s. We were unable to locate a transition-state geometry where the H atom migration could be stabilized by the metal surface. Our computational efforts to trace a pathway by simply scanning the separation between the α-hydrogen and the γ-carbon for the allenyl-to-methylacetylide isomerization do render a transition state in Figure 10, however, with a barrier height that is ~50 kcal/mol higher than the experimental value. Sophisticated transition-state searches are invited.

4. Discussion

4.1. Comparisons with C_3H_3—Metal Complexes. Here, we demonstrated a propargyl−allenyl−methylacetylide isomerization process on a metal surface. Such a series of rearrangements has been quite rare even in transition-metal chemistry. Gladysz[29] and co-workers, during attempts to prepare allene complexes of rhenium, demonstrated a propargyl to allenyl rearrangement, that is, $Cp(NO)(PPh_3)Re(\eta^1\text{-}CH_2C\equiv CH) \rightarrow Cp(NO)(PPh_3)Re(\eta^1\text{-}CH=C=CH_2)$. The same studies also provided a further example where treatment of an allene precursor $Cp(NO)(PPh_3)Re(\eta^2\text{-}CH_2=C=CH_2)$ with the stronger base methyllithium gave $Cp(NO)(PPh_3)Re(\eta^1\text{-}CH=C=CH_2)$, a σ-bound allenyl complex that was readily transformed to a methylacetylide complex $Cp(NO)(PPh_3)Re(\eta^1\text{-}C\equiv CCH_3)$ on treatment with HBF_4 and ^{t}BuOK, via an intermediate η^2-bound alkyne complex $Cp(NO)(PPh_3)Re(\eta^2\text{-}CH\equiv CCH_3)^+$. However, such an intramolecular allenyl−acetylide rearrangement via a stepwise protonation−deprotonation process is accessible only in solvents. The only literature precedent for a concerted [1,3]-hydrogen shift at a coordinated allenyl ligand was reported by Doherty et al.,[30]

(26) Kershen, K.; Celio, H.; Lee, I.; White, J. M. *Langmuir* **2001**, *17*, 323–328.
(27) Hilberty, P. C.; Shaik, S. *Theor. Chem. Acc.* **2005**, *114*, 169–181.
(28) Ananikov, V. P.; Musaev, D. G.; Morokuma, K. *Organometallics* **2005**, *24*, 715–723.
(29) Pu, J.; Peng, T.-S.; Arif, A. M.; Gladysz, J. A. *Organometallics* **1992**, *11*, 3232–3241.
(30) Doherty, S.; Elsegood, M. R. J.; Clegg, W.; Ward, M. F.; Waugh, M. *Organometallics* **1997**, *16*, 4251–4253.

involving a binuclear iron complex $[Fe_2(CO)_6(\mu\text{-}PPh_2)\{\mu\text{-}\eta^1{:}\eta^2\text{-}CH{=}C{=}CH_2\}]$ with its C_3H_3 ligand transformed into a bridging acetylide $\mu\text{-}\eta^1{:}\eta^2\text{-}C{\equiv}CCH_3$.

Trinuclear metal complexes present themselves as bonding models for "surface" bound C_3H_3 species. The allenyl moiety, as a ligand, has been found to be η^1-bonded through C_α to one metal and η^2-bonded through $C_\alpha{=}C_\beta$ and $C_\beta{=}C_\gamma$ to the other two metals, adopting a bent $\mu_3\text{-}\eta^1{:}\eta^2{:}\eta^2$ geometry.[4] In our study, the chemisorbed allenyl on a surface shows a doubly bridging $\mu_2\text{-}\eta^1$ coordination mode in which the triangle defined by the three close-packed silver atoms is bisected by the almost linear C=C=C backbone. Being highly unsaturated and isoelectronic with CO, acetylide anions ($^-$:C≡C−H or $^-$:C≡C−R) are expected to demonstrate a diversity of bonding possibilities in transition-metal complexes.[31] Like metal carbonyls, terminal and bridging modes are all well-known. For an acetylide ligand bound to trinuclear metal centers, the most common bonding modes are either $\mu_3\text{-}\eta^2\text{-}(\perp)$ or $\mu_3\text{-}\eta^2\text{-}(\parallel)$ where the C≡C unit bridges perpendicularly or parallel to an M−M vector.[32] Here, we found that the methylacetylide group resides almost vertical to the triangular metal plane and binds to the silver atoms in an asymmetric $\mu_3\text{-}\eta^1$ face-capping geometry. This mode of coordination as compared to the well-behaved on-top configuration is quite novel but not unprecedented. For example, tricopper(I)[33] and trisilver(I)[34] complexes containing $\mu_3\text{-}\eta^1$ acetylide groups were reported in the literature. The description of the bonding in these M_3−C≡C−R moieties often refers to an electron-deficient four-center two-electron (4c−2e) σ-type interaction. NPA as implemented in the Gaussian 03 code was performed to give better insight into the metal−ligand bond nature. In our $Ag_{22}(14,8)$−C≡C−CH_3 calculation, the respective atomic charges on the α-carbon and the three nearest silver atoms are revealed to be −0.834 and (+0.268, +0.159, and +0.159), shown in Figure 10. The strong ionic characters suggest that the metal−acetylide bonds are held together via substantial dative/electrostatic interactions. To neutralize its charge, methylacetylide thus acts as a two-electron donor toward a total of three metal centers. This preference for the high coordination sites has been observed for other polar ligands, such as alkoxides and thiolates.[35]

4.2. Isomerization of Metal-Bound Allyl vs Propargyl. Allyl (−CH_2−CH=CH_2) and propargyl (−CH_2−C≡CH) groups share a three-carbon, 1,3-alternate unsaturation nature. Transition metals form both η^1- and η^3-allyl complexes, and the two modes of metal−C_3H_5 bonding can be interconverted. In η^3-allyl complexes, the metal lies out of the C_3 plane below the centroid of the triangle defined by these carbon atoms, and this type of π-bonded allyl was also identified on Cu and Ag surfaces.[20,36] Furthermore, Celio and White found a unique $\eta^3\text{-}\eta^1\text{-}\eta^3$ pathway linking the exo and endo conformations of the π-bonded allyl groups on the same surfaces in the presence of coadsorbed halogens.[20] However, there has been no precedent for a [1,3]-hydrogen shift between η^1-allyl and η^1-propenyl (M−CH_2−CH=CH_2 → M−CH=CH−CH_3) found on metal surfaces. Metal η^3-propargyls are generally referred to as η^3-propargyl/allenyl because these two resonance forms are often fluxional. Unlike their η^3-allyl counterpart, the metal is coplanar with the C_3 skeleton, and the η^3-bonding mode is less prevalent than the η^1-mode.[4] In metal complexes, the η^1- to η^3-propargyl/allenyl conversion was found to be kinetically less favored than the corresponding allyl conversion, occurring about 9 times slower at ambient temperature.[37] It is thus not surprising that our study detected no evidence for the π-bonded η^3-propargyl/allenyl or an $\eta^1\text{-}\eta^3\text{-}\eta^1$ movement, and only η^1-allenyl form was isolated and characterized spectroscopically at 200−250 K surface temperatures. We report here the first example of a metal surface-catalyzed isomerization of σ-bonded η^1-allenyl to η^1-methylacetylide through a [1,3]-hydrogen shift (M−CH=C=CH_2 → M−C≡C−CH_3). Maitlis et al. proposed a mechanism for the Fischer−Tropsch synthesis where the chain growth is initiated by methylene insertion into the metal−vinyl bond to give surface ally, and then the ally must isomerize to alkenyl which in turn combines with more methylene.[38] Here, the recognition that unsaturated C_3 ligands other than ally can rearrange their internal multiple bond may support the role of the isomerization step in carbon−carbon chain growth processes.

4.3. Methyl Substitution and Halogen Effects. Although at first glance the methyl group substitution on a propargyl moiety (−*CR_2−C≡CH, R = CH_3) appears to be a relatively minor alteration, and has proven to be a useful tactic for supporting the proposed allenyl formation (*CR_2=C=CH−) mechanism, the alkyl-for-hydrogen substitution might have other profound influences on such polarizable π-systems, and further investigation is warranted. The employment of Cl−$(CH_3)_2$C−C≡CH has certainly assisted us in arguing for the hydrogenation processes; however, the chloro-for-bromo replacement, a compromise due to the unavailability of Br−$(CH_3)_2$C−C≡CH, is not entirely uncontroversial. For example, the relatively robust C−Cl bond should be hard to break on a coinage metal surface because the C−X bond activation rates decrease in the order of C−I > C−Br > C−Cl. Lin and Bent reported that for *alkyl* chlorides the surface reaction switches from molecular desorption to C−X bond dissociation between C_6 and C_7, while the transition is between C_2 and C_3 for bromides.[39] The gas-phase bond dissociation energies for Cl−CH_2CH_3 and Br−CH_2CH_3 are 80 vs 68 kcal/mol; however, they decline to 68 vs 54 kcal/mol for C_3 *allylic* Cl−CH_2CH=CH_2 and Br−CH_2CH=CH_2.[40] Thus, several research groups utilized *allyl* chloride as precursor to generate adsorbed C_3H_5 fragments below 200 K on Ag(111) and Ag(110) under UHV conditions.[19,20] Along this line, we expect that a portion of the adsorbed *propargyl* chloride can also branch out into the C−Cl bond scission route at 200 K, evidenced indirectly by the detection of subsequent hydrogenation products, rather than molecular desorption, in TPD (Figure 9). Moreover, all the surface chemistry reported here is carried out in the presence of codeposited halogens, and chlorine, subsurface Cl in particular, is known to exhibit salient electronic effects on the activity and selectivity of Ag-based catalysis.[41] Therefore, its influence on adsorbate stabilities and mechanism

(31) Carty, A. J. *Pure Appl. Chem.* **1982**, *54*, 113–130.
(32) Mays, M. J.; Raithby, P. R.; Sarveswaran, K.; Solan, G. A. *J. Chem. Soc., Dalton Trans.* **2002**, 1671–1677.
(33) Gamasa, M. P.; Gimeno, J.; Lastra, E.; Aguirre, A.; Garcia-Granda, S. *J. Organomet. Chem.* **1989**, *378*, C11–C14.
(34) Aroz, R.; Mohr, F.; Cerrada, E.; Tiekink, E. R. T.; Laguna, M. *Polyhedron* **2006**, *25*, 3066–3070.
(35) Diez, J.; Gamasa, M. P.; Gimeno, J. *Polyhedron* **1995**, *14*, 741–745.
(36) Celio, H.; Smith, K. C.; White, J. M. *J. Am. Chem. Soc.* **1999**, *121*, 10422–10423.
(37) Casey, C. P.; Underiner, T. L.; Vosejpka, P. C.; Gavney, J. A., Jr.; Kiprof, P. *J. Am. Chem. Soc.* **1992**, *114*, 10826–10834.
(38) Maitlis, P. M.; Long, H. C.; Quyoum, R.; Turner, M. L.; Wang, Z.-Q. *Chem. Commun.* **1996**, 1–8.
(39) Lin, J.-L.; Bent, B. E. *J. Phys. Chem.* **1992**, *96*, 8529–8538.
(40) Fox, M. A.; Whitesell, J. K. *Organic Chemistry*, 2nd ed.; Jones and Bartlett Publishers: London, 1997.
(41) Lambert, R. M.; Cropley, R. L.; Husain, A.; Tikhov, M. S. *Chem. Commun.* **2003**, 1184–1185.

definitely exists, but fortunately is not serious enough to change the major results, involving triple-bond migration, self-hydrogenation, and C—C bond formation steps.

5. Conclusions

Propargyl bromide shows intriguing thermal chemistry on a Ag(111) surface where three isomeric structures of the C_3H_3 moieties and their mutual conversions are identified unambiguously. The thermal stabilities of these various C_3H_3 forms follow the trend: $Ag—CH_2—C{\equiv}CH < Ag—CH{=}C{=}CH_2 < Ag—C{\equiv}C—CH_3$. In particular, the allenyl to methylacetylide transformation via a [1,3]-hydrogen shift, rarely found in organometallic and surface science literature, is observed for the first time on a metal surface. Using α,α-dimethyl-substituted propargyl species and RAIRS, we are able to recognize the identities for the hydrogenation products resulting from the normal propargyl at various reaction temperatures. Hydrogenation is totally selective to allene and propyne, and the hydrogen is regioselectively added to the α-carbon, namely allenyl + H → allene and methylacetylide + H → propyne. This is different from the common pathway for metal—allenyl or metal—propargyl complexes when reacted with proton (electrophile) in the solution phase where reduction of the allenyl and propargyl species affords acetylene and allene, respectively. Propargyl is prone to have its remote C≡C functionality migrate from a terminal to an internal position, driven by the higher stability of the metal acetylide. The triple bond structures are thus virtually interchangeable in the presence of metals, and this isomerization route represents an interesting case in electronic communication along metal—polyunsaturated chains. [1,3]-Hydrogen shifts and [1,3]-sigmatropic rearrangements, common reactions in organic chemistry, have proven to play mechanistically interesting roles in this model C_3H_3 heterogeneous system. Utilization of this cascade of rearrangements to catalytically transform metal propargyl into metal acetylide may have applications in the synthesis of polyunsaturated materials.

Acknowledgment. We thank the National Science Council of the Republic of China for financial support under Contract No. 95-2113-M-110-016. We are also grateful to the National Center for High-Performance Computing for computer time and facilities.

JA803509Y